PHYSICAL REVIEW B **81**, 121410(R) (2010)

Patterns in strained-layer heteroepitaxy: Beyond the Frenkel-Kontorova model

Joshua D. Howe,[1,2] Prateek Bhopale,[1] Yogesh Tiwary,[1] and Kristen A. Fichthorn[1,2]
[1]*Department of Chemical Engineering, The Pennsylvania State University, University Park, Pennsylvania 16802, USA*
[2]*Department of Physics, The Pennsylvania State University, University Park, Pennsylvania 16802, USA*
(Received 2 February 2010; published 15 March 2010)

The second layer of Ag on Pt (111) is experimentally observed to form a striped dislocation pattern with Ag stripes alternating between fcc and hcp stacking. We address the origins of the stripes with a combination of density-functional theory and Monte Carlo simulations. We find that this dislocation pattern is driven by electronic and anisotropic substrate-mediated interactions associated with the Shockley surface state on Ag (111). Our simulations reveal the quantum mechanical underpinnings of strain-relief patterns, previously described phenomenologically by the classical Frenkel-Kontorova model that is widely used to describe such systems.

DOI: 10.1103/PhysRevB.81.121410 PACS number(s): 68.55.J−, 68.35.Ct, 68.35.Gy

Understanding the phenomena and forces that dictate self-assembly is of considerable current interest. One driving force for self-assembly at surfaces is the strain that develops in epitaxial layers when atoms of one material are deposited onto the surface of another material. This strain can lead, for example, to the formation of quantum dots via the Stranski-Krastanov growth mode in lattice-mismatched semiconductor systems.[1–4] In metal heteroepitaxy,[5–12] as well as on some pure metal surfaces,[13–16] intricate dislocation patterns form as a consequence of interfacial strain. From a fundamental point of view, the patterns that form in strained epitaxial layers are often understood in terms of the classical Frenkel-Kontorova (FK) model,[17] where the adatom-adatom interaction potential dictates a different lattice constant than the periodic adatom-substrate potential. To minimize the energy of the strained adlayer, some adatoms do not reside exactly in minima of the surface potential and dislocations are formed. Although the FK model has been applied to describe the structures observed experimentally for various homoepitaxial and heteroepitaxial systems,[18–21] we find that an alternate model is appropriate in at least some cases.

We consider the patterns that form when Ag is deposited onto Pt (111). Experimental studies with scanning-tunneling microscopy (STM) show that while the first complete monolayer (ML) of Ag on Pt (111) assumes a pseudomorphic structure, the second layer forms a network of alternating fcc and hcp stripes.[7] Upon annealing at 800 K, the striped phase reconstructs to form a trigonal network.[7,12] In this work, we address the origins of these dislocation patterns with a combination of first-principles calculations based on density-functional theory (DFT) and Monte Carlo (MC) simulations. Our work indicates that the dislocation patterns in this system are driven by substrate-mediated interactions that are electronic and quantum mechanical in origin, in contrast to the classical picture of the FK model.

The Ag (111) surface possesses a Shockley surface state that can mediate interactions between adsorbed atoms. As originally predicted by Lau and Kohn,[22] this long-range oscillatory interaction decays with adsorbate separation d as d^{-2} and has a period related to the Fermi wave vector k_F. More recently, Hyldgaard and Persson[23] refined Lau and Kohn's expression to include a phase shift δ_F and their expression takes the form

$$\Delta E_{pair}(d) \cong -\epsilon_F\left(\frac{2\sin(\delta_F)}{\pi}\right)^2\frac{\sin(2k_Fd+2\delta_F)}{(k_Fd)^2}, \qquad (1)$$

where ϵ_F is the Fermi energy relative to the minimum in the surface band. While STM studies corroborate Eq. (1) for adsorbates on *unstrained* Cu (111) (Refs. 24 and 25) and Ag (111) (Ref. 25) surfaces, our studies indicate that deviations from Eq. (1) occur for a *strained* Ag (111) surface.[26] We used DFT to quantify the pair interaction between two Ag adatoms on a compressed Ag (111) surface with the lattice constant for Pt to serve as a model for one pseudomorphic adlayer of Ag on Pt (111). While the details of these calculations are presented elsewhere,[26] we summarize the essential aspects here.

Figure 1 shows a map of the pair interaction between atoms placed at various distances from a central adatom. We obtained the pair interaction for separations ranging from the first to the 53rd neighbor, a range of over 2 nm, and found that this interaction is primarily electronic in origin. In particular, pair interactions due to relaxation of the substrate are negligible.[26] Further, we investigated various trio interactions and found that these are small compared to the pair interac-

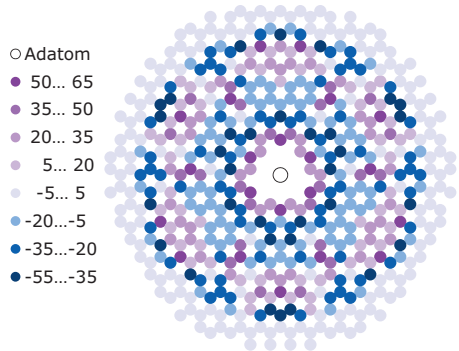

FIG. 1. (Color) Pair potential (in meV) for the interaction of a central adatom (open circle) with a second adatom on various possible fcc and hcp binding sites at distances ranging from the third to the 53rd neighbor. The interaction energies for the first and second neighbors have values of −196.3 and −136.3 meV, respectively, and are not shown for clarity.

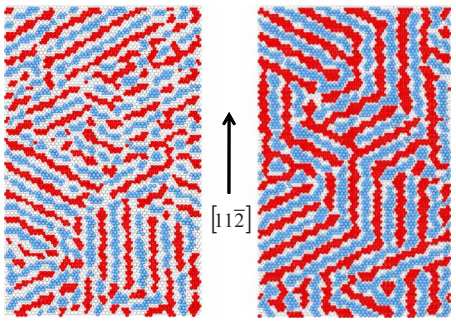

FIG. 2. (Color online) Snapshots of simulated Ag adlayers at coverages of (a) 0.5 and (b) 0.67 ML. Second-adlayer Ag atoms adsorbed on fcc sites are shown in red (dark) and atoms on hcp sites are shown in blue (lighter). First-adlayer Ag atoms are shown in white (lightest).

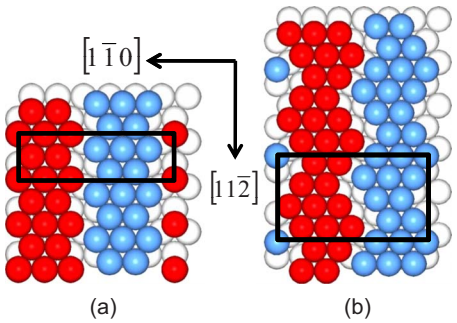

FIG. 3. (Color online) Two possible unit cells for the striped pattern at θ=0.833 ML: (a) ($\sqrt{3}\times6$) and (b) ($2\sqrt{3}\times6$) unit cell. Color scale is the same as Fig. 2.

tion, so pair interactions dominate.[26] In an average sense, the pair interaction in Fig. 1 exhibits concentric rings that alternate between attraction and repulsion, as would be predicted by Eq. (1). We fit angularly averaged interactions from Fig. 1 to Eq. (1) using values of k_F=0.28 Å^{-1} and ϵ_F=0.662 eV that emerge from independent band structure calculations.[26] This fit yields $\delta_F=0.45\pi$ and is satisfactory for interactions beyond the third neighbor—at shorter separations, direct chemical bonding dominates the interactions.[26] This implies [cf., Eq. (1)] that the period of the oscillatory interaction is $\lambda_F/2$=11 Å, where $\lambda_F=2\pi/k_F$, consistent with the average spacing between attractive and repulsive regions in Fig. 1. However, it is evident that the pair interaction in Fig. 1 contains significant radial and angular structure not predicted by Eq. (1). Below, we show that this anisotropy plays a crucial role in governing the structure of a strained Ag adlayer.

To understand the ramifications of the interactions in Fig. 1 for pattern formation in strained layers, we performed Metropolis MC simulations of Ag adatoms on an fcc (111) surface representative of 1 ML of Ag on Pt (111). The surface is discretized into an array of fcc and hcp binding sites and adatom interactions are described by the potential in Fig. 1 (including first- and second-neighbor interactions). In a previous DFT study,[27] we found that the binding energy for adatoms on fcc sites is only slightly higher (by less than ~3 meV) than that for hcp sites so we neglect the slight energetic preference for epitaxial registry. We examined Ag fractional coverages θ between 0.15 and 0.833 ML [i.e., the actual coverages on the Pt (111) surface would be 1.15 and 1.833 ML, respectively] at temperatures between 0 and 3500 K. We simulated between 800 (θ=0.15) and 4442 (θ=0.833) Ag atoms and tested various possible lattice sizes to correctly accommodate the periodicity of the Ag adlayers. For each set of conditions, we obtained results for at least two runs beginning with different initial conditions. Additionally, we checked for hysteresis effects by heating and cooling the simulated lattices, to ensure that the simulated structures were representative of equilibrium for the given temperature.

Figure 2 shows snapshots of the Ag adlayer at θ=0.50 (a) and θ=0.67 (b), where we see that a striped phase has formed in which stripes run along the $\langle 11\bar{2}\rangle$ direction with three different orientations. Interestingly, atoms alternate occupancy between fcc and hcp binding sites in neighboring stripes. Below θ=0.3, isolated islands occur with well defined sizes and our previous work focused on characterizing these.[28,29] The islands merge into stripes at coverages above 0.3, as can be seen in Fig. 2(a), where islands still occur and coexist with stripes. The interstripe spacing in the $\langle 1\bar{1}0\rangle$ direction normal to the stripes is constant at ~8.5 Å and independent of coverage: as can be seen by comparing Figs. 2(a) and 2(b), the vacant space between stripes decreases and the stripe width increases with increasing coverage.

It is difficult to simulate coverages much higher than 0.7 due to the declining efficiency of the MC method. Thus, to explore possible stripe configurations at the highest coverages, we constructed various striped patterns and calculated their total energies. We performed MC simulations of these patterns on small lattices to confirm their stability. For the given stripe density, the maximum possible Ag atom coverage is 0.833 and assuming equal occupancy of fcc and hcp stripes there are two possible unit cells depicted in Fig. 3. The first of these, shown in Fig. 3(a), has a ($\sqrt{3}\times6$) unit cell with domain walls oriented along the $\langle 11\bar{2}\rangle$ direction, as proposed experimentally,[7] and the second, shown in Fig. 3(b), has "miniherringbone" stripes with smooth $\langle 1\bar{1}0\rangle$ domain walls and a ($2\sqrt{3}\times6$) unit cell. Our calculations indicate that the ($\sqrt{3}\times6$) unit cell in Fig. 3(a) is energetically favored by 7 meV/atom.

Since the oscillatory interactions in Fig. 1 have a period governed by the Fermi wavelength,[26] we look for this characteristic length in the simulated striped patterns. We note that, while the interstripe distance of ~8.5 Å (along the $\langle 1\bar{1}0\rangle$ direction) does not correlate well with λ_F, the stripes in Fig. 3(a) are five atoms wide (~11.2 Å)—a distance very close to $\lambda_F/2$—in two of the three equivalent $\langle 1\bar{1}0\rangle$ directions, while the stripes in Fig. 3(b) are five atoms wide in one of three $\langle 1\bar{1}0\rangle$ directions. Thus, key structural aspects of the stripes are governed by the Fermi wavelength.

In the analogous experimental study by Brune *et al.*,[7] a striped pattern oriented along the $\langle 11\bar{2}\rangle$ direction was identified that had a ($\sqrt{3}\times p$) unit cell, with $p=14\pm1$ and ($p-1$) adatoms for p substrate atoms. The fact that we find a

smaller (but similar) unit cell than experiment may indicate that the Fermi wavelength is smaller in our calculations than in experiment. In a previous study, we found that strain can significantly influence the value of λ_F and that this quantity decreases with increasing compression of the lattice.[26] For example, on *unstrained* Ag (111) λ_F is estimated to be 76 Å,[25] which is significantly larger than what we find here. The DFT results in Fig. 1 were obtained on an Ag slab in which the lattice constant was compressed by 4.61% relative to the DFT value for bulk Ag,[26] while the experimental compression in this system is 4.2%.[30] The greater compression employed in our study is consistent with a surface state that is shifted further below the Fermi level with a larger value of k_F and, hence, with a smaller period for the stripes than that observed experimentally. Some experimental support for this idea can be seen in the work of Neuhold and Horn,[31] who showed that a 0.5% tensile strain of Ag (111) can shift the surface state above the Fermi level. It is also worth mentioning that our simulated stripes are similar in their orientation and fcc-hcp alternation to those seen on Au (111),[13,14] which is also a compressed surface with a Shockley surface state.

In the experimental unit cell, the occupancy of fcc sites (16 out of 26 atoms in the unit cell) is higher than that for hcp sites, while we have equal occupancy here. At least part of this discrepancy stems from our neglect of the energetic difference (which we find to be small but favorable to fcc binding) between fcc and hcp binding sites. Although three-body interactions are small compared to pair interactions in this system,[26] these (and higher-order many-body interactions) may also contribute to a preference for epitaxial registry of the stripes.

Despite the above discrepancies, there are remarkable similarities between our simulated adlayers and those seen experimentally.[7] First, we reproduce the $\langle 11\bar{2}\rangle$ orientation and the alternation between fcc and hcp stacking. We reproduce the narrow and dilute domain-wall structure seen in experiment.[7] In a recent study, Pushpa *et al.*[21] developed an FK model for this system based on DFT calculations for the Ag-substrate interaction and a short-range empirical potential for the Ag-Ag interaction. They performed an exhaustive search for various phases that could occur as a function of two empirical parameters characterizing the Ag-Ag interaction. While they found a phase with alternating fcc and hcp stripes along $\langle 11\bar{2}\rangle$, their model predicts a gradual transition from fcc to hcp stripes, with wide domain walls involving height variation in the Ag atoms, in contrast to the narrow domain walls and minimal height variation observed here and in experiment.

In experiments, a trigonal dislocation network is observed after annealing the stripes.[7,12] We did not observe this pattern, despite extensive attempts. Pushpa *et al.* did observe a triangular pattern in their FK model[21]—although this did not closely resemble experiment. There is evidence from low-temperature STM that dislocations in the trigonal network include atoms in the Pt (111) surface.[12] Here, we assume that all atoms below the second adlayer are fixed to Pt (111) lattice sites, which may explain the difference. It is also possible that our λ_F is too small and that an energetic preference for fcc registry is needed to observe the trigonal network.

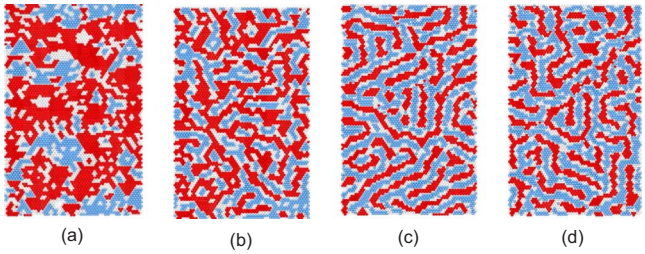

FIG. 4. (Color online) Snapshots of simulated Ag adlayers at θ=0.67 ML and T=340 K using the DFT pair potential for the first x neighbor interactions and Eq. (1) for x+1 through 53rd-neighbor interactions, where (a) x=3, (b) x=10, (c) x=19, and (d) x=31. Color scale is the same as Fig. 2.

We now turn to the origins of our simulated striped patterns, which lie in the interactions shown in Fig. 1. Since (as discussed above) an angular average of the interactions in Fig. 1 can be reasonably well fit to Eq. (1), one might naively expect that an *isotropic* potential based on Eq. (1) could also produce the striped phase. Using this isotropic potential (plus DFT interactions for first-through third-neighbor interactions), we ran MC simulations and observed compact and randomly placed regions of fcc and hcp occupancy separated by smooth $\langle 1\bar{1}0\rangle$ edges, as shown in Fig. 4(a). These calculations indicate that angular variations in the interactions in Fig. 1, which represent a deviation from theory,[22,23] play an essential role in stabilizing the striped phase.

We also conducted a series of simulations to determine if there are any specific interactions among those in Fig. 1 that give rise to the striped phase. In these simulations a short-ranged portion of the interactions was given by DFT, while the remaining long-ranged portion was based on the fit to Eq. (1). These simulations indicate that alternating fcc and hcp stripes along the $\langle 11\bar{2}\rangle$ direction do not occur to any significant extent until the DFT interactions extend from the first to the 19th neighbor, as shown in Figs. 4(b) and 4(c). Furthermore, smooth $\langle 1\bar{1}0\rangle$ domain walls persist until DFT interactions are used for the first 30 nearest-neighbor interactions, where $\langle 11\bar{2}\rangle$ domain walls emerge, as shown in Fig. 4(d). Finally, the stripes do not form the extended networks, shown in Fig. 2 and seen in experiment,[7] until interactions up to and beyond the 50th nearest-neighbor are included. These studies indicate that *all* of the interactions in Fig. 1 are important and act in a cooperative manner to produce the striped phase.

In summary, we find that long-range anisotropic interactions mediated by surface-state electrons can facilitate the formation of dislocation networks in heteroepitaxial adlayers. Although existing theory predicts these interactions are isotropic and can successfully describe them on unstrained surfaces,[22–25] our calculations show that these interactions become anisotropic on strained surfaces and that this anisotropy is essential in promoting the formation of dislocation networks. Our simulations reveal the quantum mechanical underpinnings of strain-relief patterns and contrast the classical FK model that has been widely used to describe such systems.

This work was sponsored by NSF Grant No. DMR-9617122.

[1] B. A. Joyce and D. D. Vvedensky, Mater. Sci. Eng. R. **46**, 127 (2004).
[2] K. Brunner, Rep. Prog. Phys. **65**, 27 (2002).
[3] J. Tersoff, C. Teichert, and M. G. Lagally, Phys. Rev. Lett. **76**, 1675 (1996).
[4] V. A. Shchukin and D. Bimberg, Rev. Mod. Phys. **71**, 1125 (1999).
[5] C. Günther, J. Vrijmoeth, R. Q. Hwang, and R. J. Behm, Phys. Rev. Lett. **74**, 754 (1995).
[6] H. Zajonz, A. P. Baddorf, D. Gibbs, and D. M. Zehner, Phys. Rev. B **62**, 10436 (2000).
[7] H. Brune, H. Röder, C. Boragno, and K. Kern, Phys. Rev. B **49**, 2997 (1994).
[8] H. Brune, M. Giovannini, K. Bromann, and K. Kern, Nature (London) **394**, 451 (1998).
[9] W. L. Ling, J. C. Hamilton, K. Thürmer, G. E. Thayer, J. de la Figuera, R. Q. Hwang, C. B. Carter, N. C. Bartelt, and K. F. McCarty, Surf. Sci. **600**, 1735 (2006).
[10] W. L. Ling, J. de la Figuera, N. C. Bartelt, R. Q. Hwang, A. K. Schmid, G. E. Thayer, and J. C. Hamilton, Phys. Rev. Lett. **92**, 116102 (2004).
[11] B. Diaconescu, G. Nenchev, J. Jones, and K. Pohl, Microsc. Res. Tech. **70**, 547 (2007).
[12] K. Aït-Mansour, A. Buchsbaum, P. Ruffieux, M. Schmid, P. Gröning, P. Varga, R. Fasel, and O. Gröning, Nano Lett. **8**, 2035 (2008).
[13] J. V. Barth, H. Brune, G. Ertl, and R. J. Behm, Phys. Rev. B **42**, 9307 (1990).
[14] A. R. Sandy, S. G. J. Mochrie, D. M. Zehner, K. G. Huang, and D. Gibbs, Phys. Rev. B **43**, 4667 (1991).
[15] M. Bott, M. Hohage, T. Michely, and G. Comsa, Phys. Rev. Lett. **70**, 1489 (1993).
[16] A. R. Sandy, S. G. J. Mochrie, D. M. Zehner, G. Grubel, K. G. Huang, and D. Gibbs, Phys. Rev. Lett. **68**, 2192 (1992).
[17] J. Frenkel and T. Kontorova, J. Phys. (USSR) **1**, 137 (1939).
[18] S. Narasimhan and D. Vanderbilt, Phys. Rev. Lett. **69**, 1564 (1992).
[19] J. C. Hamilton, Phys. Rev. Lett. **88**, 126101 (2002).
[20] J. C. Hamilton and S. M. Foiles, Phys. Rev. Lett. **75**, 882 (1995).
[21] R. Pushpa, J. Rodríguez-Laguna, and S. N. Santalla, Phys. Rev. B **79**, 085409 (2009).
[22] K. H. Lau and W. Kohn, Surf. Sci. **75**, 69 (1978).
[23] P. Hyldgaard and M. Persson, J. Phys.: Condens. Matter **12**, L13 (2000).
[24] J. Repp, F. Moresco, G. Meyer, K. H. Rieder, P. Hyldgaard, and M. Persson, Phys. Rev. Lett. **85**, 2981 (2000).
[25] N. Knorr, H. Brune, M. Epple, A. Hirstein, M. A. Schneider, and K. Kern, Phys. Rev. B **65**, 115420 (2002).
[26] W. Luo and K. A. Fichthorn, Phys. Rev. B **72**, 115433 (2005).
[27] K. A. Fichthorn and M. Scheffler, Phys. Rev. Lett. **84**, 5371 (2000).
[28] K. A. Fichthorn, M. L. Merrick, and M. Scheffler, Appl. Phys. A: Mater. Sci. Process. **75**, 17 (2002).
[29] K. A. Fichthorn, M. L. Merrick, and M. Scheffler, Phys. Rev. B **68**, 041404(R) (2003).
[30] H. Brune, K. Bromann, H. Röder, K. Kern, J. Jacobsen, P. Stoltze, K. Jacobsen, and J. Nørskov, Phys. Rev. B **52**, R14380 (1995).
[31] G. Neuhold and K. Horn, Phys. Rev. Lett. **78**, 1327 (1997).